Improving Modeling of MEMS-IMUs Operating in GNSS-denied Conditions

Stebler, Yannick; Guerrier, Stéphane; Skalud, Jan; Victoria-Feser, Maria-Pia

Improving Modeling of MEMS-IMUs Operating in GNSS-denied Conditions

Yannick Stebler[1], Stéphane Guerrier[2], Jan Skaloud[1], and Maria-Pia Victoria-Feser[2]

[1]*Geodetic Engineering Laboratory, École Polytechnique Fédérale de Lausanne* (EPFL), Switzerland
[2]*Research Center for Statistics, Faculty of Economics and Social Sciences, University of Geneva*, Switzerland

Yannick Stebler obtained in 2008 a M.Sc. in Geomatics engineering from EPFL. He is currently Ph.D. student in the Geodetic Engineering Laboratory of EPFL under the supervision of Dr. Jan Skaloud. His research focuses on the fusion of redundant MEMS-based inertial sensors for navigation and sensor error modeling.

Stéphane Guerrier obtained in 2008 a M.Sc. in Geomatics engineering from EPFL for his work on the integration of redundant MEMS-IMUs with GPS. He's now working as a Ph.D student and teaching assistant in the Research Center for Statistics, Faculty of Economics and Social Sciences of the University of Geneva. His research concentrates on model selection in mixed linear models and on the estimation of stochastic processes.

Jan Skaloud is a lecturer and senior scientist at EPFL. He holds Ph.D. and M.Sc. Degrees in Geomatics Engineering from Canada (The University of Calgary) and Dipl. Ing. Degree from CVUT (Prague, Czech Rep.). His areas of research are navigation, sensor integration and calibration, mobile mapping and remote sensing.

Maria-Pia Victoria-Feser is Professor of Statistics in the Research Center for Statistics, Faculty of Economics and Social Sciences of the University of Geneva. She holds a Ph.D. in Econometrics and Statistics from the University of Geneva and she has been lecturer at the Statistics Department of the London School of Economics (1993-1996) and assistant professor at the Faculty of Psychology and Educational sciences of the University of Geneva (2000-2004). Her research and publications are in fundamental statistics, with specialization in robust statistics, parametric density estimation, extreme value modelling, generalised linear models, latent variables models.

***Abstract*—Stochastic modeling is a challenging task for low-cost inertial sensors whose errors can have complex spectral structures. This makes the tuning process of the INS/GNSS Kalman filter often sensitive and difficult. We are currently investigating two approaches for bounding the errors in the mechanization. The first is an improved modeling of stochastic errors through the superposition of several Auto-Regressive (AR) processes. A new algorithm is presented based on the Expectation-Maximization (EM) principle that is able to estimate such complex models. The second approach focuses on redundancy through the use of multiple IMUs which don't need to be calibrated *a priori*. We present a synthetic IMU computation in which the residuals are modeled by a single ARMA model. The noise power issued from the residuals is then continuously estimated by a GARCH model, which enables a proper weighting of the individual devices in the synthetic IMU.**

I. Introduction

The combination of inertial navigation with Global Navigation Satellite Systems (GNSS) through and Extended Kalman filter (EKF) is a well known and accepted technique in navigation. During periods of GNSS gaps or poor GNSS signal quality, inertial navigation operates in coasting mode, i.e. the navigation states are determined independently from GNSS data, the reason for which the overall performance become strongly dependent on the errors corrupting inertial signals. Generally, the resulting navigation error increases with time. In the last years, the use of Micro-Electro-Mechanical System (MEMS)-based sensors has significantly decreased the cost, size, weight and power consumption of IMUs. However, their high noise level and complex error structure (in-run biases and scale factors) significantly degrade the final Position-Velocity-Attitude (PVA) provided by the navigation filter. For such setup, the improvement of navigation can be made at two levels.

The first is achieving correct *a priori* calibration of the individual inertial sensors, i.e. the gyroscopes and accelerometers, that sets the deterministic and stochastic structure of the error signature. Commonly used error models for MEMS-based sensors are composed of a bias and a scale factor, both containing deterministic (e.g. axes misalignment) errors which are compensated through physical models, and random components which are described by stochastic processes. Commonly used stochastic processes are Gaussian White Noise (WN), Random Walk (RW), first-order Gauss-Markov (GM), bias instability (BI), rate ramp (RR) or quantization noise (QN). These are included in the State-Space Model (SSM) forming the error-states in the navigation EKF. The questions of which stochastic processes to use for best describing the stochastic part of the individual sensors in IMUs and which parameter values to use in the SSM/EKF lead to the challenging task of filter tuning. We suggest that in many cases inertial sensor errors may be best modeled by superposing multiple stochastic processes. However, we reckon that the estimation of the parameters of such models might become difficult when using classical tools like signal Auto-Correlation Function (ACF) analysis or the Allan Variance (AV) technique. Although AV is a well-established technique for identifying processes and estimating their parameter(s), it works reasonably well only for processes which are clearly identifiable and separable in the spectral domain and not subject to spectral ambiguity [1]. The particular case of the GM parameter (i.e. the inverse correlation time β and the driving noise power σ^2_{GM}) estimation is difficult/impossible

to carry out using ACF or AV analysis when mixed with some other process(es). In practice, the values of these parameters are approximated through *ad hoc* tuning, rely on manufacturers' specifications or experience [2].

The second level of improvement is the use of Redundant IMUs (RIMUs). IMU signals can be combined through several integration schemes [3, 4]. The benefits of using redundant sensors are multiple. First, the noise level of the overall system can be reduced and defective sensors detected and isolated. This improves the accuracy of autonomous navigation, and hence system performance in GNSS-poor condition [5]. Second, the gyroscope and accelerometer noise levels can be estimated directly from the data and provide hence a better view on the reality. This is an interesting feature with respect to the fact that sensor stochastic error modeling is often performed on error signal acquired in static conditions in spite of the supposition that the error behavior may vary as a function of environmental conditions applied to the sensors [6, 7], such as the temperature, electrical power, magnetic fields or the dynamics. Moreover, if no reliable *a priori* calibration of the invidual sensors is available, the direct noise estimation capability of RIMUs enables performing a continuous estimation of the RIMU system noise level.

This paper introduces solutions at both levels by providing a synthetic description of their principles and empirical results. Sec. II focuses on the first level where a new calibration procedure is presented based on a constrained form of the Expectation-Maximization (EM) algorithm. This estimates parameters of multiple superposed stochastic processes [8]. The particular case of GM process parameter estimation is difficult to be handeld by AV and is therefore used as a concrete example. An application of the algorithm on a real data set is provided and its effect on improving the trajectory estimation is demonstrated. Sec. III deals with the second level through a new experimental setup that allows studying errors in dynamical conditions. It focuses on the potential of instantly estimating varying noise levels in synthetic IMUs (S-IMU), a particular RIMU mechanization architecture. For that, we use Auto-Regressive Moving-Average (ARMA) models for modeling the correlated part of the noise, and Generalized Auto-Regressive Conditional Heteroskedasticity (GARCH) models for continuously estimating the residual variance for each individual sensor forming the S-IMU [5]. Finally, Sec. IV closes the paper by providing perspectives and concluding remarks

II. Prior Determination of Error Structure

Signals issued from MEMS-based inertial sensors are affected by random errors whose spectral structure is often complex. The modeling of such errors may be achieved by superposing several stochastic processes, such as wide band noise (i.e. WN) and (several) GM processes, which can be considered as first-order Auto-Regressive (AR) models [9]. In this section, we propose an algorithm that is able to estimate parameters of such model types when analyzing the time series of error signal (often collected in static conditions). The algorithm is based on a constrained form of the EM principle. For a proper understanding of the method, the notion of SSM is recalled before moving to the algorithm principle.

A. Linear Dynamical System

A discrete Linear Time-Invariant (LTI) dynamical system can be described by the following SSM:

$$\mathbf{x}_{t+1} = \mathbf{\Phi}\mathbf{x}_t + \mathbf{w}_t + \boldsymbol{u}_t \tag{1}$$

with measurements

$$z_{t+1} = \mathbf{H}\mathbf{x}_{t+1} + v_{t+1} \tag{2}$$

where $\mathbf{x}_t$ is the $p \times 1$ system state vector at time t, $\mathbf{\Phi}$ is the discrete $p \times p$ transition matrix, $\mathbf{w}_t$ is a random forcing function such that $\mathbf{w} \sim \mathcal{N}(\mathbf{0}, \mathbf{Q})$, $\mathbf{u}_t$ is a $r \times 1$ deterministic input vector, z_t is an element at time t of the $l \times 1$ measurement vector $\mathbf{z}$, $\mathbf{H}$ is the $l \times p$ design matrix which maps the true state space $\mathbf{x}_t$ into the observed space, and v_t is an element of the $l \times 1$ noise vector $\mathbf{v}$ such that $\mathbf{v} \sim \mathcal{N}(\mathbf{0}, \mathbf{R})$. The initial state $\mathbf{x}_1$ is assumed to be a normal random vector with mean vector $\boldsymbol{\mu}$ and $p \times p$ initial covariance matrix $\mathbf{\Sigma}$ (*i.e.* $\mathbf{P}_1^1$).

B. SSM for Inertial Sensor Errors

For modeling random errors, we have to construct a discrete SSM from the differential equations describing the process dynamics. Lets define $\boldsymbol{\theta} \in \mathbf{\Theta}$ as the set of SSM parameters which characterize model (1)-(2):

$$\boldsymbol{\theta} = \{\mathbf{u}, \mathbf{\Phi}, \mathbf{Q}, \mathbf{R}, \mathbf{H}, \boldsymbol{\mu}, \mathbf{\Sigma}\} \tag{3}$$

In our case, some elements of the SSM parameters are not known and have to be estimated, while others have to be kept fixed.

Suppose for example that we want to model the observed sensor error signal $\mathbf{z}$ that is a mixture of WN, RW, GM processes and a deterministic drift with slope ω. The discrete process equations are provided in Tab. I.

Process	**Equation**	$w_t \sim \mathcal{N}(0, q)$
GM	$x_{t+1} = (1 - \beta\Delta t)x_t + \Delta t w_t$	$q = 2\beta\sigma_{GM}^2$
RW	$x_{t+1} = x_t + w_t$	$q = \sigma_{RW}^2$
WN	$x_t = w_t$	$q = \sigma_{WN}^2$

TABLE I: Equations governing the stochastic processes. Note that the GM equation is a first-order approximation.

Typically, the individual model parameters are impossible to estimate using classical AV. The state-space representation of this model in first-order approximation is given by

$$\begin{aligned} \mathbf{x}_{t+1} &= \begin{bmatrix} 1 - \beta\Delta t & 0 \\ 0 & 1 \end{bmatrix} \mathbf{x}_t + \mathbf{w}_t + \begin{bmatrix} 0 \\ \omega\Delta t \end{bmatrix} \\ z_{t+1} &= \begin{bmatrix} 1 & 1 \end{bmatrix} \mathbf{x}_{t+1} + v_{t+1} \end{aligned}$$

such that $\mathbf{w}_t \sim \mathcal{N}(\mathbf{0}, \mathbf{Q})$ with

$$\mathbf{Q} = \begin{bmatrix} 2\beta\sigma^2_{GM} & 0 \\ 0 & \sigma^2_{RW} \end{bmatrix}$$

and $v_t \sim N(\mathbf{0}, \mathbf{R})$ with

$$\mathbf{R} = \begin{bmatrix} \sigma^2_{WN} \end{bmatrix}$$

The aim of sensor calibration is to estimate the unknown parameter set

$$\boldsymbol{\theta} = \{\beta, \sigma^2_{GM}, \sigma^2_{RW}, \sigma^2_{WN}, \omega\}$$

from the signal $\mathbf{z}$. Such problem typically requires that some elements in the involved matrices must remain fixed while others are estimated. For example, all elements in $\mathbf{\Phi}$ excepting $1 - \beta\Delta t$ must remain fixed. In $\mathbf{u}$, the first element must stay null, while only the diagonal of $\mathbf{Q}$ contains free elements. Since all the elements of $\mathbf{H}$ are fixed, this matrix does not need to be estimated. Note that $\mathbf{u}$ can be determined separately, e.g. by a Least-Squares (LS) regression [8].

Since the (log) likelihood function $\log L(\boldsymbol{\theta}|\mathbf{z}_t, \mathbf{x}_t)$ is a highly nonlinear and complicated function, the estimation of the SSM parameters through its maximization is in general quite challenging [10]. [11] proposed the EM algorithm originally developed in [12] to maximize $\log L(\boldsymbol{\theta}|\mathbf{z}_t, \mathbf{x}_t)$. In navigation, the EM algorithm has mainly been used for estimating $\mathbf{Q}$ and $\mathbf{R}$ in which all parameter elements are estimated [13, 14]. However, when using EM for more complex SSMs such as in our case, where additional SSM matrices are included in $\boldsymbol{\theta}$, a constrained version of the EM needs to be used.

C. Constrained Expectation-Maximization (EM)

The aim of the EM is to find $\boldsymbol{\theta}$ that maximizes $\log L(\boldsymbol{\theta}|\mathbf{z}_t, \mathbf{x}_t)$. As $\mathbf{x}_t$ is unobservable in our case, it is replaced by the "complete-data" likelihood $\mathbf{\Psi} = \mathbb{E}\left[\log L(\boldsymbol{\theta}|\mathbf{z}_t, \mathbf{x}_t)\right]$ whose full expression is given in [11, 15]. The EM algorithm switches iteratively between an Expectation (E-)step and a Maximization (M-)step [16]. On the $(j+1)$th iteration, the E- and M-steps are defined as follows:

E-Step. Calculate $Q\left(\boldsymbol{\theta}|\boldsymbol{\theta}^{(j)}\right)$, where

$$Q\left(\boldsymbol{\theta}|\boldsymbol{\theta}^{(j)}\right) = \mathbb{E}\left[\log L(\boldsymbol{\theta}^{(j)}|\mathbf{z}_t, \mathbf{x}_t)\right] = \mathbf{\Psi}^{(j)}$$

M-Step Choose $\boldsymbol{\theta}^{(j+1)}$ to be any value of $\boldsymbol{\theta} \in \mathbf{\Theta}$ which belongs to:

$$\boldsymbol{\theta}^{(j+1)} = \underset{\boldsymbol{\theta}\in\mathbf{\Theta}}{\operatorname{argmax}}\, Q\left(\boldsymbol{\theta}|\boldsymbol{\theta}^{(j)}\right)$$

The E- and M-steps are iteratively repeated until some convergence criterion is fulfilled (e.g. until $|L\left(\boldsymbol{\theta}^{(j+1)}|\mathbf{z}_t, \mathbf{x}_t\right) - L\left(\boldsymbol{\theta}^{(j)}|\mathbf{z}_t, \mathbf{x}_t\right)| < \epsilon$ for some arbitrarily small amount ϵ) [16]. In the E-step, the expected states together with their associated covariance matrices are computed using a Kalman smoother such that they could be considered fixed in the M-step where $\mathbf{\Psi}^{(j)}$ will be maximized [11]. In the M-step, the parameter vector is updated to $\boldsymbol{\theta}^{(j+1)}$ by finding the parameters that maximize $\mathbf{\Psi}^{(j)}$ considering the smoothed states and covariances obtained in the E-step as fixed. For doing that, the expression yielded by $\mathbf{\Psi}^{(j)}$ is minimized by computing the partial derivatives with respect to $\boldsymbol{\theta}^{(j)}$ and setting them to zero. The results of these derivatives for the classical unconstrained case can be found in many articles like [11, 15]. However, the work in [15, 17] provides the way of constraining elements in the matrices of $\boldsymbol{\theta}$. The update equations for each individual parameter of $\boldsymbol{\theta}$ in the M-step of the constrained EM algorithm, together with the practical issues encountered when applying it to inertial sensors, can be found in [8].

D. Algorithm Validation through Simulations

We apply the constrained EM algorithm on 200 realizations of a synthetic error signal $\mathbf{z}$ of length 6000 generated under the model of the example in Sec. II-B. The following parameter values are used:

$$\boldsymbol{\theta} = \{0.008, 0.25, 10^{-8}, 0.09, 10^{-4}\}$$

The initial parameters are set to:

$$\boldsymbol{\theta}^{(0)} = \{10^{-4}, 10^{-6}, 10^{-10}, 2.5 \cdot 10^{-7}, 0\}$$

The results of the 200 runs are shown in Fig. 1. Note that $\mathbf{u}$ has been estimated beforehand by LS regression. This improves the estimation of the remaining parameters in EM as shown in [8]. The estimation appears to be biased, specially for the inverse correlation time of GM and RW strength. This is due to the difficulty of clearly separating them in the spectral space. We now study the restitution of AV plots by the parameter set $\hat{\boldsymbol{\theta}}$ estimated via EM. We computed the AV for 20 realizations issued from 3 (among the 200 runs) randomly selected solutions $\hat{\boldsymbol{\theta}}$ (see Fig. 2). The effect of the bias in some parameters is visible through the systematic overbounding in the middle part of the AV sequences. However, despite the estimated parameters do not reconstruct the error structure *exactly*,

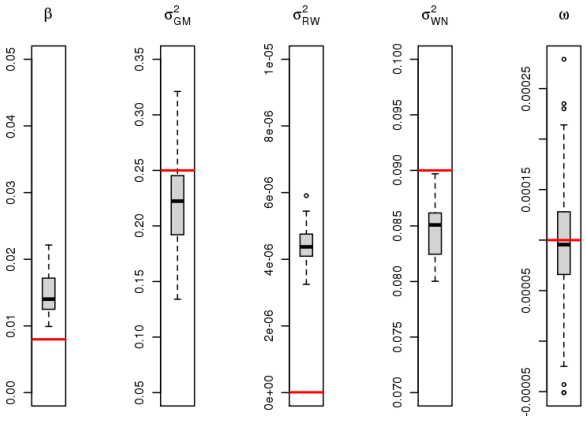

Fig. 1: Performance of the EM algorithm where $\mathbf{u}$ has been removed by LS for 200 simulations of a mixture containing WN, GM, RW and a drift. The true parameters are marked by horizontal lines.

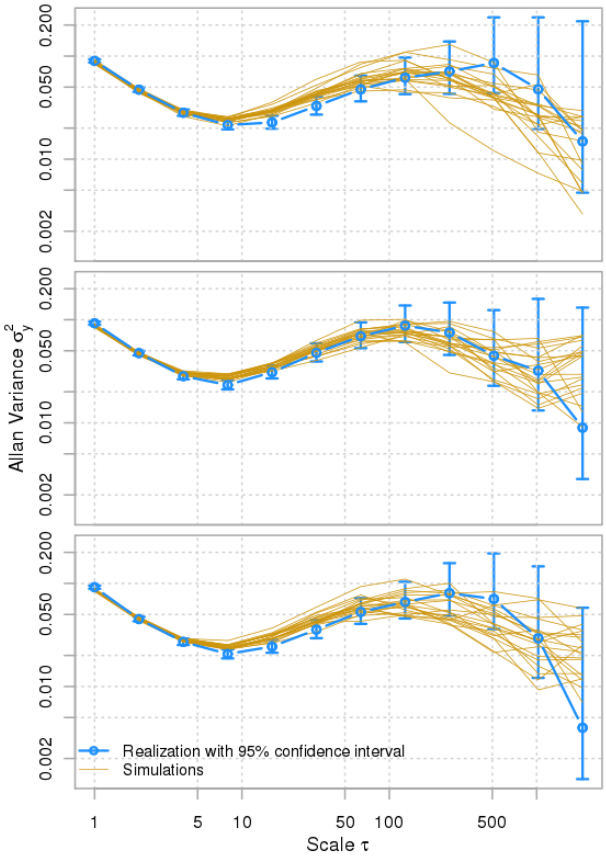

Fig. 2: Results for the signals containing GM, RW, and WN mixed with a drift. Each panel shows the AV of one realization issued from $\boldsymbol{\theta}$ (thick curve) and 20 simulations driven from the corresponding estimated parameter sets $\hat{\boldsymbol{\theta}}$ (thin curves).

it provides an tight overbound of the true AV signal (i.e. when considering the 95% confidence interval associated with the AV estimation of the true signal), similarly to the methodology proposed in [18].

E. Application on a Real Signal

We apply the constrained EM algorithm on signals issued from a tactical-grade IMU (*IMAR-FSAS* [19]). Three hours long static data were collected in constant temperature conditions at a sampling frequency of 100 Hz. The observed variations in signal output are considered as errors which can be used as observations z_t in Eq. (2). The AV plots revealed that the gyroscope error signals are mainly composed of a white noise and thus present no need for more sophisticated modeling. However, the AV plot of accelerometer errors (thick curve in Fig. 3 for Y-axis accelerometer) show a more complex error structure. The analyses are similar for the X- and Z-axis sensors and are therefore not shown here. Since the slopes of the linear parts in the thick AV curve do not correspond to any of the theoretical processes identifiable through AV, we choose to model this error by superposing two GM processes and a

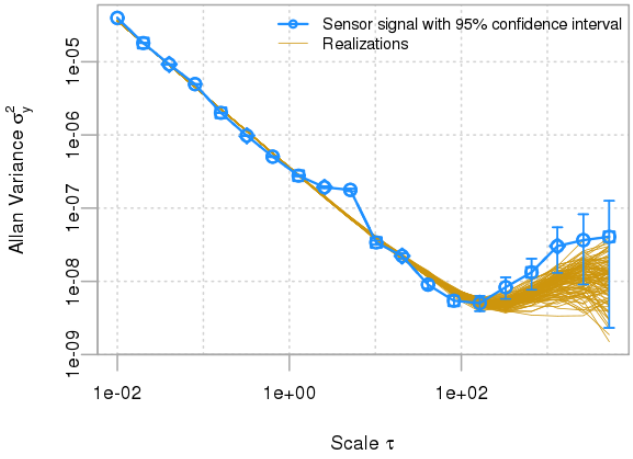

Fig. 3: Results of the estimation of 2 GM processes and a WN process applied on the *IMAR-FSAS* Y-axis accelerometer error signal. The figure shows the AV of 100 realizations issued from $\hat{\boldsymbol{\theta}}$ (thin curves) and the AV of the sensor signal (thick curve).

WN. Such model can be written as:

$$\begin{aligned} \mathbf{x}_{t+1} &= \begin{bmatrix} 1-\beta_1\Delta t & 0 \\ 0 & 1-\beta_2\Delta t \end{bmatrix} \mathbf{x}_t + \mathbf{w}_t \\ z_{t+1} &= \begin{bmatrix} 1 & 1 \end{bmatrix} \mathbf{x}_{t+1} + v_{t+1} \end{aligned}$$

such that $\mathbf{w}_t \sim \mathcal{N}(\mathbf{0}, \mathbf{Q})$ with

$$\mathbf{Q} = \begin{bmatrix} 2\beta_1\sigma^2_{GM,1} & 0 \\ 0 & 2\beta_2\sigma^2_{GM,2} \end{bmatrix}$$

and $v_t \sim N(\mathbf{0}, \mathbf{R})$ with

$$\mathbf{R} = \begin{bmatrix} \sigma^2_{WN} \end{bmatrix}$$

The goal is to estimate the parameter set:

$$\boldsymbol{\theta} = \{\beta_1, \beta_2, \sigma^2_{GM,1}, \sigma^2_{GM,2}, \sigma^2_{WN}\}$$

from the signal $\mathbf{z}$. The estimated values for the parameters obtained with the EM algorithm are:

$$\hat{\boldsymbol{\theta}} = \{0.0004, 0.10, 4 \cdot 10^{-8}, 10^{-8}, 3.6 \cdot 10^{-5}\}$$

where the units of the β and variances are $[1/s]$ and $[(m/s^2)^2]$, respectively. The estimation quality is illustrated in Fig. 3 in which AV plots of 100 realizations issued from the estimated set $\hat{\boldsymbol{\theta}}$ (thin curves) are compared with that of the real sensor signal (thick curve). The estimated power level of WN appears to fit well the real signal (left part of AV curve). Although staying within the estimated intervals of confidence, the long-term errors modeled by the two GM processes match the signal AV sequence only approximately (right part of AV curve). This can be explained by the following reasons, which highlight the limitations of the constrained EM algorithm:

- The identification of the GM parameters within a process containing much higher power of WN is difficult and induce very long convergence time in the likelihood-maximization step.
- When some parameters to be estimated are of small magnitude, an accumulation of numerical imprecision

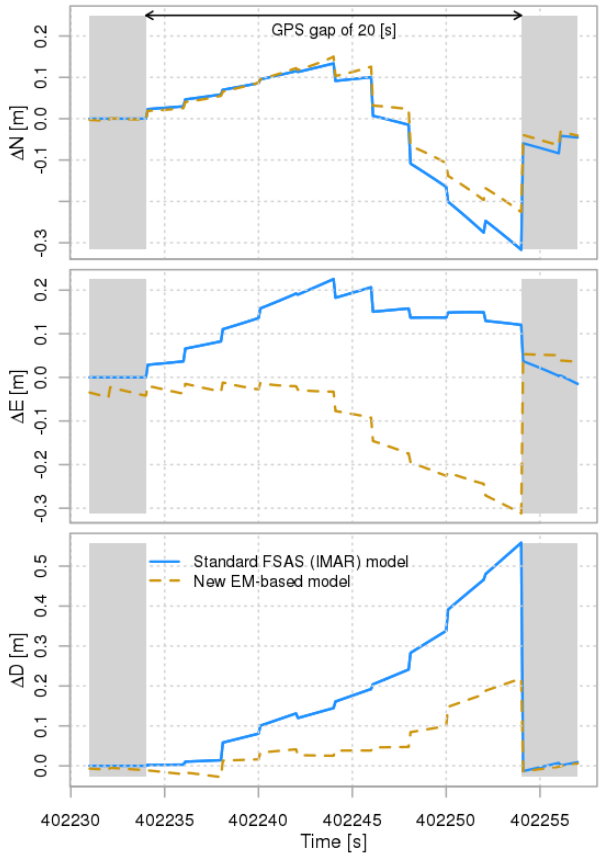

Fig. 4: Position errors along North (first panel), East (second panel) and Down (third panel) component occuring during the 20s-long GPS outage when using the traditional error model (full curves) and the new model (dotted curves) in the EKF.

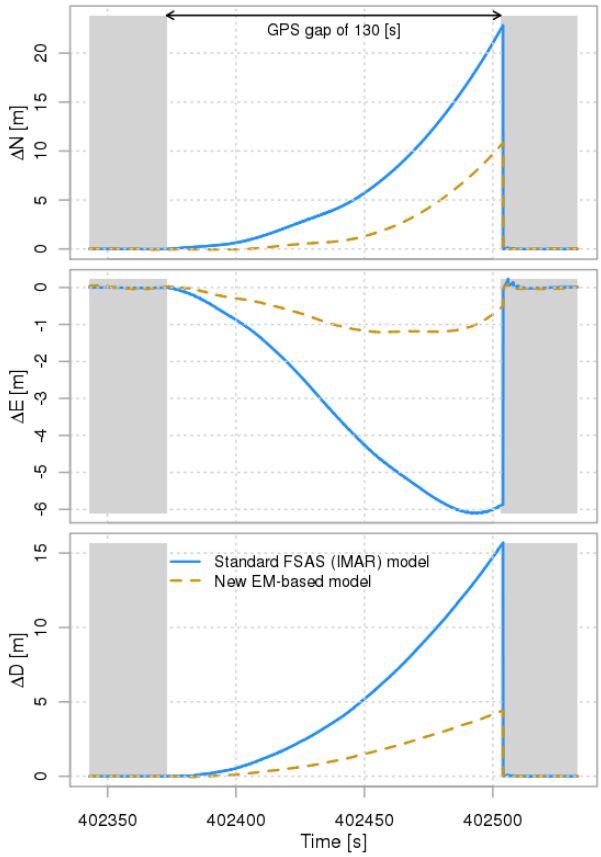

Fig. 5: Position errors along North (first panel), East (second panel) and Down (third panel) component occuring during the 130s-long GPS outage when using the traditional error model (full curves) and the new model (dotted curves) in the EKF.

in many iteration may influence the quality of estimation.

- Using longer time series would most likely improve the uncertainty of parameter estimation, especially for processes with long memory. Indeed, a longer signal may improve the observation of the underlaying long-term processes (right part in the AV plot), in other words, decreasing the 95% confidence intervals in this region, while improving the estimation of the GM parameters by the EM algorithm.

In the sequel, we analyze the impact of the estimated model on the INS/GNSS integration via optimal forward Kalman filtering and backward smoothing. For that, the *IMAR-FSAS* IMU was mounted together with a high-grade dual-frequency GPS receiver (*JAVAD*) on a car, and the motion was sampled at 100 Hz and 10 Hz, respectively (see Fig. 6). The carrier-phase GPS observations were double-differenced in post-processing to yield high-precision (cm-level) GPS positioning. These have been combined with the inertial observations in a loosely-coupled EKF. To highlight the impact of proper stochastic modeling, we introduced artificially two outages in GPS solutions of different duration, at times where good and reliable GPS solutions were actually available and can be used as a reference. During these outages, the navigation solution is solely dependent on inertial navigation, meaning that the residual systematic errors affecting these signals are integrated with time. We then recomputed the INS/GPS trajectory using the traditional *IMAR-FSAS* stochastic error model provided by the manufacturer, and compared it to the EKF/smoothed solution using the EM-estimated model. In both cases we compared the positioning differences (N-E-D) with respect to the reference trajectory (the one without gap) and take them for errors.

The first 20s-long outage has been introduced in a time during which the car was turning in a roundabout. Fig. 4 depicts the processed position differences along each axis when using the traditional *IMAR-FSAS* model (full curves) and the new model (dotted curves). Except for the East component, the new model significantly decreased the trajectory errors based on inertial coasting during this period.

The second outage was longer (about 130s) and affected a period in which the car was moving on a straight road, and its acceleration varied. As shown in Fig. 5, the filtered trajectory errors were better bounded at the end of this outage (by a factor of 2-4) when using the new model. Indeed, the maximum observed difference could be decreased from 23 m to 10 m along the North component, from -6 m to -1.2 m along the East component, and from

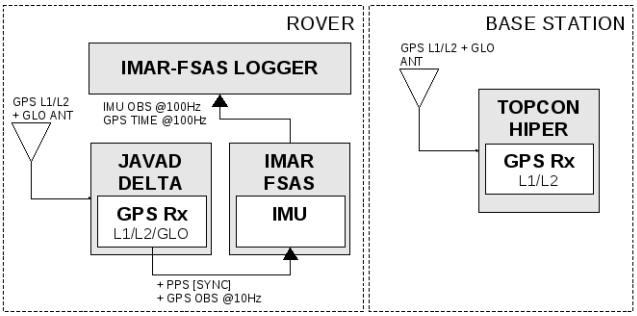

Fig. 6: Instrumental setup used for the experiment dedicated to the individual sensor error modeling.

16 m to 4.2 m along the vertical component.

III. Adaptive Modeling through Synthetic IMU

The computation of an S-IMU together with the extended and geometrically-constrained IMU mechanization, are ways of achieving redundancy in inertial navigation [3, 4, 20, 21]. An S-IMU is formed by fusing the observations of several IMUs before being introduced to the INS/GNSS integration based on single IMU mechanization (Fig. 9). In such a simple setup, traditional scheme of INS/GNSS integration is kept while defective sensors can be detected prior to strapdown navigation. Furthermore, realistic noise level and covariance terms for EKF can directly be estimated [3, 20]. However, the compound error-states estimated by the EKF cannot be fed back to the individual IMUs. This means that the EKF has to deal with a synthetic observation set which is affected by compound errors issued from the individual sensors. Since the structure of the compound errors can be complicated, the filter design (i.e. the choice of the error processes in the SSM) may not be straigtforward in such a case. Note that a corollary to that statement is that the computation of an S-IMU may be relevant for designs in which arrays of non-calibrated sensors have to be used. Therefore, we propose anticipating this issue and propose simplifying the error structure of the individual sensors through an adequate one-step removal of the correlated error components. We model these errors as an ARMA process and estimate its coefficients by whitening the residuals for each sensor. Subsequently, this allows optimal weighting of the individual signals in the S-IMU computation. Indeed, the weights will be given by the ARMA residual variance which can be estimated for each period of time by a GARCH model requiring an unpredictable signal as input (i.e. the whitened residuals). In such a scenario, the synthetic signal noise level is reduced and a simplified error model can be assumed in the EKF used for S-IMU/GNSS integration. The next section describes some practical issues related to the realization of an S-IMU, before focusing on ARMA-GARCH modeling and estimation.

A. Redundant IMU Realization

The RIMU system under test was built from three IMUs of the same type (XSens MTx MEMS-IMUs) and one XSens

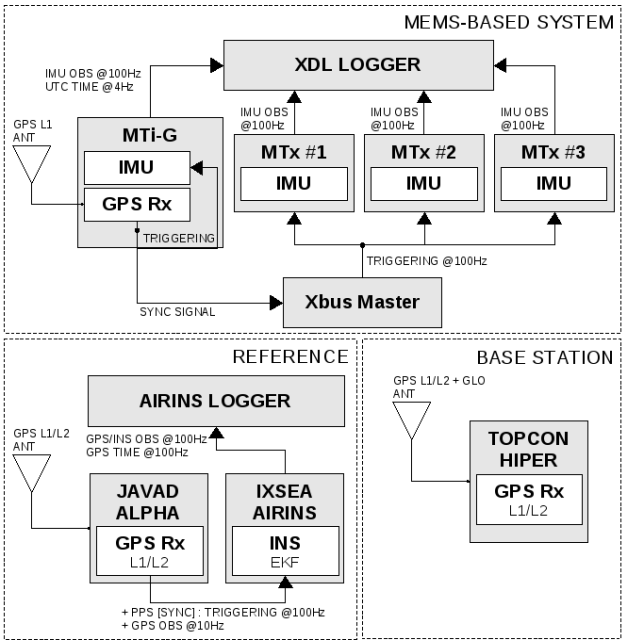

Fig. 7: Instrumental setup used for the realization and study of an S-IMU (MEMS-based system).

MTi-G unit (containing a GPS receiver and a MEMS-IMU), all sampling at 100 Hz. Reference signals were issued from an Ixsea Airins INS (noise $< 0.0015\,\mathtt{deg}/\sqrt{\mathtt{Hr}}$, drift $< 0.01\,\mathtt{deg}/\mathtt{Hr}$), combined with a geodetic grade Javad Alpha L1/L2 GPS rover receiver (sampling at 10 Hz), and a Topcon Hiper Pro L1/L2 GPS base receiver (sampling at 5 Hz), both used for computing a double-differenced carrier-phase GPS solution. The reference data was post-processed through Kalman filtering yielding compensated inertial signals. All IMUs were sampling simultaneously at 100 Hz and all observations were aligned in a common spatial and temporal frame (see Fig. 7). The individual IMU measurements were transformed from the associated sensor frames to a unique body frame (b-frame) defined as the Airins instrumental frame. The relation between the transformed gyroscope observations $\boldsymbol{\omega}_{ib}^{b}$ and the signals expressed in the kth sensor frame (k-frame) is given by

$$\boldsymbol{\omega}_{ik}^{k} = \mathbf{C}_{b}^{k}\boldsymbol{\omega}_{ib}^{b} \tag{4}$$

where $\boldsymbol{\omega}_{ik}^{k}$ is the angular rate signal measured by sensor k in the k-frame, and $\mathbf{C}_{b}^{k}$ is the direction cosine matrix expressing the relative orientation between the b- and k-frames. The transformed accelerometer signal $\mathbf{f}^{b}$ can be obtained through the following equation:

$$\mathbf{f}^{k} = \mathbf{C}_{b}^{k}\mathbf{f}^{b} + \dot{\boldsymbol{\omega}}_{ib}^{b} \times \mathbf{r}^{k} + \left(\boldsymbol{\omega}_{ib}^{b} \times \boldsymbol{\omega}_{ib}^{b} \times \mathbf{r}^{k}\right) \tag{5}$$

where $\mathbf{f}^{k}$ is the specific force signal measured by sensor k, and $\mathbf{r}^{k}$ is the eccentricity vector relating the origins of the b- and k-frames. All sensors were mounted on a manufactured platform for which $\mathbf{C}_{b}^{k}$ and $\mathbf{r}^{k}$ are precisely known. Beside the spatial alignment, the realization of the S-IMU requires the less straightforward definition and calibration of the timing relationship at two levels: the first level is the synchronization of the IMUs forming the RIMU system, while the second is the time alignment of

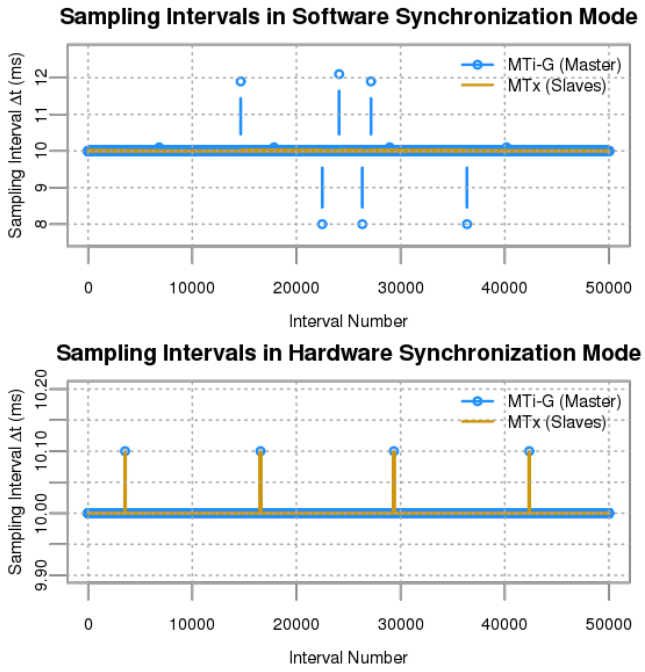

Fig. 8: Demonstration of relative timing: MTi-G and MTx (at 100 Hz) sampling intervals in software (upper panel) and hardware (lower panel) syncronization mode.

the RIMU with the reference system. Since both systems include GPS yielding access to a globally available timing and synchronization framework, GPS time will be used as common absolute time frame at both levels.

A RIMU logging and synchronization software, named XDL, has been developped for achieving data alignement within the RIMU system in real time. XDL implements two options of time synchronization. The first is the *Software Sync* mode in which time synchronization is performed by using the operating system (OS) time as a timing base. The time offset between GPS time (coming from MTi-G data packets) and the OS time is continuously estimated to calibrate the timing based on sample counter interval (in the MTx devices). However, relying on data packets can be problematic due to variable processing speeds and transmission delays of the IMU packets on the sensor end. Furthermore, indeterminate timing behaviors from software-based synchronization on a non real time OS can induce timing errors higher than 10 milliseconds [22]. The second implemented option is the *Hardware Sync* mode in which a periodic sync pulse delivered by the MTi-G serves as base for sampling all IMU measurements. This hardware-generated pulse is aligned to UTC time and is used to correct the internal MTi-G clock bias. The pulse marks the time instance at which the MTi-G samples the internal sensors. This sync signal is brought as input through a manufactured cable to the XBus Master device supervising and triggering the MTx devices. The absolute timing of the IMU messages is performed by the XDL software which exploits available GPS time messages and the guaranteed (by hardware) synchronous MTx internal sensor triggering. This relative timing capability is demonstrated in Fig. 8 which compares the varying sampling intervals of the MTx devices (slaves) with respect to the MTi-G (master) in the *Software Sync* mode (upper panel). These are perfectly aligned in *Hardware Sync mode* (lower panel in Fig. 8). where the syncronization precision is below 1 millisecond.

B. Direct Noise Estimation

Let $\{z_{t,k},: \ t = 1, 2, \ldots, N\}$, $k = 1, 2, \ldots, K$ be a set of N observations issued from one sensor type (i.e. an accelerometer or a gyroscope) of the K IMUs forming the S-IMU. Each observation $z_{t,k}$ is affected by an error $y_{t,k}$ with its corresponding variance $\sigma^2_{t,k}$.

Theoretically, at a given time t, the best estimate of the expected value $\hat{z}_t$ can be computed as a weighted average of the K measurements. Assuming homogeneous measurements (i.e. constant $\sigma_{t,k}$, $k = 1, \ldots, K$), its power $\hat{\sigma}^2_t$ can be derived as

$$\hat{\sigma}^2_t = \sum_{k=1}^{K} w^2_k \hat{\sigma}^2_{t,k} = \frac{\hat{\sigma}^2}{K} \tag{6}$$

where w_k are the weigthing factors, and $\hat{\sigma} = \hat{\sigma}_{t,k}$, $\forall k$.

However, the research in [5] revealed that the assumption of giving equal weights to all sensors is not realistic since the noise powers across sensors may vary significantly. In [5], an ARMA model was used for modeling the auto-correlated signal part while GARCH models were introduced as direct noise estimation technique for S-IMUs able to estimate changes of sensor variances.

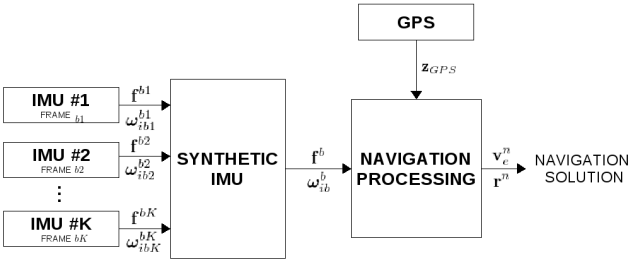

Fig. 9: Principle of INS/GNSS integration using an S-IMU.

C. ARMA-GARCH Modeling and Sensor Weighting

The research in [5, 7, 23, 24] demonstrated the presence of colored noise in MEMS-based IMUs. In case of S-IMU, ARMA models can be used to remove the auto-correlated noise components when forming the synthetic observations [9, 25, 26]. Nevertheless, once ARMA models are applied, the residuals may not be homoskedastic as shown in [5], and their variance needs to be estimated via GARCH models. In the sequel, we briefly outline this methodology that is described in [5], before focusing on empirical testing.

Lets define $\mathbf{\Omega}_t$ as the information set at time t and $\{\epsilon_t : t = 1, 2, \ldots, N\}$ as the set of observations to be modeled using a GARCH process, the residuals of an ARMA in our context. Then, the best prediction for $t + 1$ at time t

is the conditional expectation $\mathbb{E}[\epsilon_{t+1}|\mathbf{\Omega}_t]$ based on $\mathbf{\Omega}_t$. In GARCH models, one assumes that the best prediction ϵ_{t+1} at t satisfies

$$\mathbb{E}[\epsilon_{t+1}|\mathbf{\Omega}_t] = \mathbb{E}[\epsilon_{t+1}]$$

Furthermore, GARCH models are based on the idea that the signal variance tends to form clusters, which implies that squared values of the residuals (i.e. ϵ_t^2) are positively correlated. Thus, ϵ_t is conditionally heteroskedastic, i.e.

$$\text{var}[\epsilon_{t+1}|\mathbf{\Omega}_t] \neq \text{var}[\epsilon_{t+1}] \tag{7}$$

We have now all prerequisites for defining a ARMA(d,h) - GARCH(p, q) model. Such model is defined as

$$y_t = \nu + \sum_{i=1}^{d} \alpha_i y_{t-i} + \sum_{i=1}^{h} \beta_i \epsilon_{t-i} + \epsilon_t \tag{8}$$

$$\sigma_t^2 = \gamma_0 + \sum_{i=1}^{p} \gamma_i \epsilon_{t-i}^2 + \sum_{i=1}^{q} \delta_i \sigma_{t-i}^2 \tag{9}$$

where $\epsilon_t \sim \mathcal{N}(0, \sigma_t^2)$. The estimation of such a model (8)-(9) is in practice a difficult task and the Quasi-Maximum Likelihood (QML) is generally used in this context. Indeed, [27] proved that under (8)-(9), the QML estimate is consistent and asymptotically normally distributed.

The selection of the appropriate orders d, h and p, q was realized based on the Akaike Information Criterion (AIC) (proposed in [28])

$$AIC = 2k - 2\ln[L(\hat{\boldsymbol{\theta}}_{ML}, \mathbf{y})]$$

where $\mathbf{y}$ is the vector containing the error samples y_t, $\hat{\boldsymbol{\theta}}_{ML}$ is the Maximum Likelihood (ML) estimate parameter vector containing the k parameters which characterize model (8)-(9):

$$\boldsymbol{\theta} = [\alpha_1, \ldots, \alpha_d, \beta_1, \ldots, \beta_h, \gamma_0, \ldots, \gamma_p, \delta_1, \ldots, \delta_q]^T \tag{10}$$

and $L(\boldsymbol{\theta}, \mathbf{y})$ its log-likelihood function which can be expressed as

$$L(\boldsymbol{\theta}, \mathbf{y}) = \prod_{t=\max(d,h)}^{N} \frac{1}{\sqrt{2\pi\sigma_t^2}} \times \exp\left[\frac{-\left(y_t - \nu + \sum_{i=1}^{d} \alpha_i y_{t-i} + \sum_{i=1}^{h} \beta_i \epsilon_{t-i}\right)^2}{2\sigma_t^2}\right]$$

In our case, an ARMA(3,2) and GARCH(1,1) was selected. Note that since QML estimation is used instead of ML in such models, the AIC is only an approximation of the prediction in this case and should be used with precaution. Using the AIC$_c$ proposed by [29] may improve this approximation but goes behond the scope of this article.

D. Results on Corrected S-IMU Computation

In practice, the true error signal $\mathbf{y}$ is unavailable and hence must be approximated by the estimated residuals

$$\hat{y}_{t,k} = z_{t,k} - \frac{1}{K}\sum_{k=1}^{K} z_{t,k} \tag{11}$$

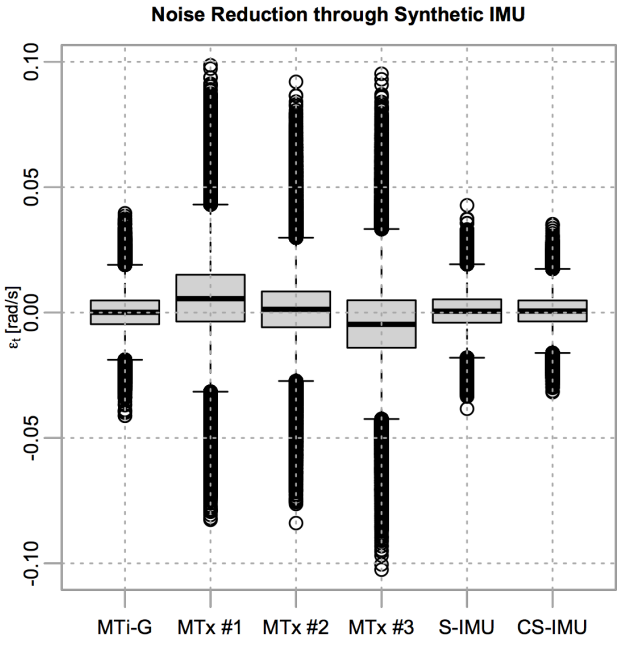

Fig. 10: Boxplot of the residuals of the Z-axis gyroscope signals of the four individual devices, the classical S-IMU, and the CS-IMU.

where $\hat{y}_{t,k}$ is the estimated residual of the kth sensor at time t. The variance estimation using the ARMA-GARCH modeling technique enables weighting the measurements issued from the individual sensors according to their estimated variances. Thus, we compute the Corrected S-IMU (CS-IMU) according to

$$\hat{z}_t = \frac{\sum_{k=1}^{K} \hat{\sigma}_{t,k}^{-2} \left(z_{t,k} - \mathbb{E}[y_{t,k}]\right)}{\sum_{k=1}^{K} \hat{\sigma}_{t,k}^{-2}} \tag{12}$$

where $\hat{\sigma}_{t,k}^2$ is the variance of the measurement error estimated with the ARMA-GARCH model at time t, i.e. an estimate of

$$\sigma_{t,k}^2 = \text{var}\left[z_{t,k} - \mathbb{E}[y_{t,k}|\mathbf{\Omega}_{t-1}]|\mathbf{\Omega}_{t-1}\right] \tag{13}$$

The conditional expectation $\mathbb{E}[y_{t,k}|\mathbf{\Omega}_{t-1}]$ can be estimated by means of $\hat{y}_{t,k}$, i.e. $\hat{\mathbb{E}}[y_{t,k}|\mathbf{\Omega}_{t-1}]$, given by

$$\hat{y}_{t,k} = \hat{\nu}_k + \sum_{i=1}^{d} \hat{\alpha}_{i,k} \hat{y}_{t-i,k} + \sum_{i=1}^{h} \hat{\beta}_{i,k} \hat{\epsilon}_{t-i,k} \tag{14}$$

and the estimated residuals of the model (8)-(9) are yielded by

$$\hat{\epsilon}_{t,k} = y_{t,k} - \hat{y}_{t,k} \tag{15}$$

In our case, the $y_{t,k}$ values are computed using the reference system described in Sec. III-A.

The resulting noise reduction of this weighting process using ARMA-GARCH model (i.e. the CS-IMU) is compared to the classical S-IMU presented in Eq. (6) as well as to the estimated residuals of each individual sensor. The Fig. 10 shows the example of the Z-axis gyroscope (similar results where obtained for the other sensors). The results show that the CS-IMU has significantly reduced noise level

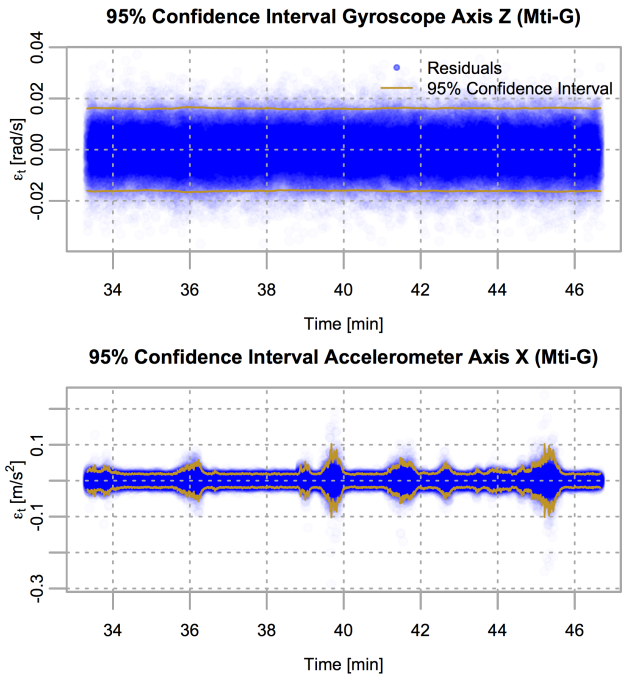

Fig. 11: Demonstration of the quality of the residual (blue circles) modeling results using the ARMA-GARCH model (brawn curve) for the Z-axis gyroscope (upper panel) and the X-axis accelerometer (lower panel) of the MTi-G IMU.

compared to the classical S-IMU. The MSE associated to the S-IMU was $4.8 \cdot 10^{-5}$ (rad^2/s^2) and was reduced to $4.0 \cdot 10^{-5}$ (rad^2/s^2) in the CS-IMU. This means that the precision gain of the CS-IMU compared to the classical S-IMU (i.e. the ratio of the root MSE) is approximately 90% for the gyroscope. Moreover, the noise level of the CS-IMU is 0.0063 (rad/s) compared to the 0.0070 (rad/s) in the S-IMU.

The quality of the variance modeling performed by the ARMA-GARCH model can be visually evaluated by having a look on Fig. 11 depicting the Z-axis gyroscope and X-axis accelerometer of the MTi-G. The accelerometer signal clearly highlights that the variances estimated with GARCH (brawn curve) seems to be appropriate to model the heteroskedacity of the residuals (blue dots).

E. Note on the INS/GNSS Integration using a Synthetic IMU

Theoreticaly, the residuals ϵ_t of model (8) are *i.i.d.* such that $\epsilon_t \sim \mathcal{N}(0, \sigma_t^2)$ if the true ARMA(d, h) parameters are known. This would imply that the resulting S-IMU signal are perfectly whitened when introduced into the EKF, and thus no additional error-states are required in the filter. In practice however, the true ARMA(d, h) parameters are unknown and hence must be estimated. The resulting estimation error implies that the estimated residuals $\hat{\epsilon}_t$ of Eq. (15) are not *i.i.d.*, meaning that some correlation may still be present. Moreover, the estimated residuals may also contain a bias since this was not considered in the model (i.e. the constant term ν of Eq. (8) was not estimated). These two issues can be handeled in the EKF by augmenting the state vector with additional error states as a random bias or a GM process for example.

IV. Conclusion and Perspectives

In this paper, we presented two solutions for dealing with the stochastic errors affecting inertial signals. The first is an *a priori* determination of error structure and its parameters separately for each sensor. An adapted algorithm based on EM was able to estimate error models in cases where classical approach based on AV fails. The proposed model was composed of several AR processes (e.g. GM processes), parameters of which were determined by the described algorithm. This method was based on the maximization of the (log) likelihood which can become complex and highly nonlinear in cases where the error structure is extremly complex. The second approach focused on merging several IMUs to form an S-IMU in which noise can be reduced. For that we studied signals under dynamical conditions with specially-developed hardware syncronization and sampling. The computation of a corrected S-IMU was performed using ARMA-GARCH technique proposed in [5] that aims removing correlated errors by weighting the individual devices. Indeed, the ARMA model provides a mean for whitening the S-IMU residuals, while the GARCH model provides adaptive estimation of noise power which is used for weighting the individual sensors in the S-IMU computation. The performance of this technique was confirmed using real signals of long duration and under dynamical conditions with respect to the classical (i.e. unweighted) S-IMU.

Further points need to be clarified in this ongoing research. First, there is still no estimation technique that can successfully determine very complex error structures such as sums of AR processes. New estimators able to deal with such situations need to be developed. Second, the ARMA-GARCH modeling has been performed on the estimated residual signals issued from the sensors themselves. A comparison with the true errors needs to be done for a proper understanding of the sensor behavior when subjected to dynamics. Finally, the impact of the removed error associated with the estimated ARMA parameters on the EKF output needs to be studied. In particular, the error model proposed for dealing with the remaining correlation and bias needs to be tested.

References

[1] C. Greenhall, "Spectral Ambiguity of Allan Variance," *IEEE Transactions on Instrumentation and Measurement*, vol. 47, no. 3, pp. 623–627, June 1998.

[2] A. Waegli and J. Skaloud, "Assessment of GPS/MEMS-IMU Integration Performance in Ski Racing," in *Proceedings of ENC-GNSS 2007 (TimeNav'07), Geneva, Switzerland*, 2007.

[3] A. Waegli, "Trajectory Determination and Analysis in Sports by Satellite and Inertial Navigation," Ph.D. dissertation, Lausanne, 2009. [Online]. Available: http://library.epfl.ch/theses/?nr=4288, http://library.epfl.ch/theses/?nr=4288

[4] J. Bancroft, "Multiple IMU Integration for Vehicular Navigation," in *Proceedings of the 22nd International Technical Meeting of The Satellite Division of the Institute of Navigation (ION GNSS 2009)*, September 2009.

[5] A. Waegli, J. Skaloud, S. Guerrier, M. Pars, and I. Colomina, "Noise Reduction and Estimation in Multiple Micro-electro-mechanical Inertial Systems," *Measurement Science and Technology*, vol. 21, p. 065201 (11 p.), 2010.

[6] S. Guerrier, "Integration of Skew-Redundant MEMS-IMU with GPS for Improved Navigation Performance," Master Thesis, École Polytechnique Fédérale de Lausanne (EPFL), Lausanne, Switzerland, June 2008.

[7] ——, "Improving Accuracy with Multiple Sensors: Study of Redundant MEMS-IMU/GPS Configurations," in *Proceedings of the 22nd International Technical Meeting of The Satellite Division of the Institute of Navigation (ION GNSS 2009)*, Savannnah, GA, USA, September 22-25 2009, pp. 3114–3121.

[8] Y. Stebler, S. Guerrier, J. Skaloud, and M. Victoria-Feser, "Constrained Expectation-Maximization Algorithm for Stochastic Inertial Error Modeling: Study of Feasibility," *Measurement Science and Technology*, vol. 22, p. 085204, August 2011.

[9] S. Nassar, K.-P. Schwarz, and N. El-Sheimy, "Modeling Inertial Sensor Errors Using Autoregressive (AR) Models," *Journal of the Institute of Navigation*, vol. 51, no. 4, pp. 259–268, 2004.

[10] R. Shumway and D. Stoffer, *Time Series Analysis and its Applications*. Springer Verlag, 2000.

[11] ——, "An Approach to Time Series Smoothing and Forecasting using the EM Algorithm," *Journal of Time Series Analysis*, vol. 3, no. 4, pp. 253–264, 1982.

[12] A. Dempster, N. Laird, and D. Rubing, "Maximum Likelihood from Incomplete Data via the EM Algorithm," *Journal of the Royal Statistical Society. Series B (Methodological)*, vol. 39, no. 1, pp. 1–38, 1977.

[13] D. Huang, H. Leung, and N. El-Sheimy, "Expectation Maximization based GPS/INS Integration for Land-vehicle Navigation," *IEEE Transactions on Aerospace and Electronic Systems*, vol. 43, no. 3, pp. 1168–1177, 2007.

[14] G. Einicke, G. Falco, J. Malos, D. Reid, and D. Hainsworth, "Parameter Estimation for Mine Navigation," in *IGNSS Symposium 2009*. Australia: International Global Navigation Satellite Systems Society, December 2009.

[15] E. Holmes, "Derivation of the EM Algorithm for Constrained and Unconstrained Multivariate Autoregressive State-Space (MARSS) models." Northwest Fisheries Science Center, NOAA Fisheries 2725 Montlake Blvd E., Seattle, WA 98112, Tech. Rep., December 2010.

[16] G. McLachlan and T. Krishnan, *The EM Algorithm and Extensions*, ser. Wiley Series in Probability and Statistics, V. Barnet, R. Bradley, N. Fisher, J. Stuart Hunter, J. Kadane, D. Kendall, D. Scott, A. Smith, J. Teugels, and G. Watson, Eds. John Wiley & Sons, Inc., 1997.

[17] L. Wu, J. Pai, and J. Hosking, "An Algorithm for Estimating Parameters of State-space Models," *Statistics & probability letters*, vol. 28, no. 2, pp. 99–106, 1996.

[18] Z. Xing and D. Gebre-Egziabher, "Modeling and Bounding Low Cost Inertial Sensor Errors," in *Position, Location and Navigation Symposium, 2008 IEEE/ION*, 2008, pp. 1122–1132.

[19] iMAR GmbH, "iIMU-FSAS [-E] Technical Documentation," March 2009. [Online]. Available: http://www.imar-navigation.de/

[20] I. Colomina, M. Gimnez, J. Rosales, M. Wis, A. Gmez, and P. Miguelsanz, "Redundant IMUs for Precise Trajectory Determination," in *XX ISPRS 2004 Congress proceedings*, Istanbul, Turkey, 2004.

[21] A. Waegli, S. Guerrier, and J. Skaloud, "Redundant MEMS-IMU Integrated with GPS for Performance Assessment in Sports," in *Position, Location and Navigation Symposium, 2008 IEEE/ION*. IEEE, 2008, pp. 1260–1268.

[22] J. Perry and J. Childs, "Timing On the Fly: Synchronization for Direct Georeferencing on Small UAVs," *Inside GNSS*, vol. 4, no. 6, pp. 34–40, November/December 2009.

[23] N. El-Sheimy, H. Hou, and X. Niu, "Analysis and Modeling of Inertial Sensors using Allan Variance," *IEEE Transactions on Instrumentation and Measurement*, vol. 57, no. 1, pp. 140–149, January 2008.

[24] H. Hou, "Modeling Inertial Sensors Errors using Allan Variance," Master's thesis, Geomatics Engineering, University of Calgary, 2004.

[25] S. Nassar, "Improving the Inertial Navigation System (INS) Error Model for INS and INS/DGPS Applications," Ph.D. dissertation, The University of Calgary, November 2003.

[26] M. Park and Y. Gao, "Error Analysis and Stochastic Modeling of Low-cost MEMS Accelerometer," *Journal of Intelligent and Robotic Systems*, vol. 46, no. 1, pp. 27–41, 2006.

[27] T. Bollerslev and J. Wooldridge, "Quasi-Maximum Likelihood Estimation and Inference in Dynamic Models with Time-varying Covariances," *Econometric reviews*, vol. 11, no. 2, pp. 143–172, 1992.

[28] H. Akaike, "A New Look at the Statistical Model Identification," *Automatic Control, IEEE Transactions on*, vol. 19, no. 6, pp. 716–723, 1974.

[29] C. Hurvich and C. Tsai, "Model Selection for Extended Quasi-likelihood Models in Small Samples," *Biometrics*, pp. 1077–1084, 1995.